This is a repository copy of *Using multiple feature spaces-based deep learning for tool condition monitoring in ultra-precision manufacturing*.

Article:

Using multiple feature spaces-based deep learning for tool condition monitoring in ultra-precision manufacturing

Chengming Shi, George Panoutsos, Bo Luo, Hongqi Liu, Bin Li and Xu Lin

Abstract—**Tool condition monitoring is critical in ultra-precision manufacturing in order to optimize the performance of the overall process, while maintaining the desired part quality. Recently, Deep Learning has been successfully applied in numerous classification tasks in manufacturing, often to forecast part quality. In this paper, a novel Deep Learning data-driven modeling framework is presented, which includes fusion of multiple stacked sparse autoencoders for tool condition monitoring in ultra-precision machining. The proposed computational framework consists of two main structures. A training model that is designed with the ability to process multiple parallel feature spaces to learn the lower-level features; and a feature fusion structure that is used to learn the higher-level features and associations to tool wear. To achieve this learning structure, a modified loss function is utilized that enhances the feature extraction and classification tasks. A dataset from a real manufacturing process is used to demonstrate the performance of the proposed framework. Experimental results and simulations show that the proposed method successfully classifies the ultra-precision machining case study with over 96% accuracy, while also outperforms comparable methodologies.**

Index Terms—**Ultra-precision manufacturing process, tool condition monitoring, deep learning, feature spaces, feature fusion.**

NOMENCLATURE

AE	Acoustic emission
ANFIS	Adaptive neuro fuzzy inference system
ANN	Artificial neural network
BPNN	Back propagation neural network
CNC	Computer numerical control
CNN	Convolutional neural network
DBN	Deep belief network
DL	Deep learning
FD	Frequency-domain
FMSSAEs	Fusion of multiple stacked sparse autoencoders
HMM	Hidden Markov model
NN	Neural network
PCA	Principal Component analysis
RMS	Root mean square
RNN	Recurrent neural network
SAE	Sparse autoencoder
SSAE	Stacked sparse autoencoder
SVM	Support vector machine
TCM	Tool condition monitoring
TD	Time-domain
v-SVR	V-support vector regression
WD	Wavelet-domain

I. INTRODUCTION

ULTRA-PRECISION manufacturing is being widely used in numerous industrial applications, such as in micro sensors, optical elements, microsatellite components, etc. Compared with traditional machining, via ultra-precision manufacturing one can achieve higher precision and better surface finish for the workpiece [1], mainly due to the diamondbased tool. Moreover, micro wear of the cutting tool has a significant influence on surface quality, which will further have a measurable impact on production efficiency and part yield rate. It has been shown that in CNC manufacturing processes tool wear significantly affects the quality of parts, hence yield rate too; by monitoring the condition of the machining tool the overall manufacturing process can be improved [2], and potentially optimized to achieve a high yield rate. Thus, there is a crucial need for methods that can accurately quantify tool condition, and offer autonomous decisions on tool life, in ultra-precision manufacturing processes.

In recent decades, many artificial intelligence methodologies have been widely used for TCM in traditional manufacturing and processing. Generally, two essentials are necessary: (1) Man-made (expert knowledge) feature extraction and design, such as the identification of statistical characteristics, FD index and wavelet coefficients. (2) Shallow-layer model development and study, such as NN, HMM, SVM, etc. [3]-[6]. Patra [7] proposed an approach based on RMS of wavelet packet coefficients captured from

AE signals and an ANN model for TCM, and indicated that RMS values of the wavelet coefficients show positive correlation to increasing drill wear. RMS and ratio of power statistics selected from AE spectra were studied by Martins et al. [5] and an ANN model was utilized in classifying tool wear states; it was shown that the features of specific frequency bands of the signal are effective at characterizing the wear condition of the tool. Ku et al. [8] researched the mapping relationship between wavelet features extracted from vibration signals and three predefined tool wear conditions based on BPNN. Statistical features in the TD and FD extracted from vibration and power signals via wavelet packet decomposition were also discussed by Niaki et al. [9] and a RNN was used for tool wear estimation; the authors studied the application of sensor information fusion in order to increase the estimation performance of the NN and the results showed that only a maximum of 13% relative error in estimating tool wear. Massol et al. [10] studied the relationship between tool condition and several features extracted from force and AE signal, and trained an ANFIS to monitor wear state. The authors developed an eXtended Takagi Sugeno (eXTS) to correlate sensory signals with several cutter health conditions, however, the accuracy of the model on unknown tool parameters is still low. Multiple AE signal features are developed by Ren et al. [11] to reveal tool condition, and an ANFIS is constructed as the wear states classifier. Meanwhile, type-2 Fuzzy Logic-based tool life estimation can evaluate the tool life along the cutting process, and also predicts the uncertainty in the tool life estimation. Qiu et al. [12] developed a hybrid approach based on HMM and RMS of wavelet packets that are used to estimate wear state in TCM. Shi et al. [13] combined principal component analysis used for feature extraction from multiple sensory signals with a least square support vector machine (LS-SVM) model to predict tool state in a broaching operation. Results showed that PCA is very efficient at capturing the underlying features and combined with LS-SVM it is possible to avoid local optima and yield good generalization properties. Fourteen TD features sensitive to tool wear were calculated by Li et al. [3] and correlation analysis was utilized for feature selection and v-SVR for tool wear condition monitoring. The authors demonstrated that the model has a good accuracy up to 96.76%, however, it was indicated that the model is only suitable for cases with small sample size. It is evident in the literature that the workflow of feature extraction followed by Machine Learning data-driven modeling has been successfully applied in TCM. However, such methodologies are only used and demonstrated in the laboratory, rather than a real manufacturing environment; which implies controlled conditions and low susceptibility to noise, uncertainty etc. In addition, it appears that the model's accuracy on tool condition identification and prognosis highly depends on the sensitivity of the extracted features [14] , which is often performed systematically, but not autonomously (via expert knowledge).

A number of significant challenges will need to be addressed if the already developed methods for TCM in traditional/standard machining processes are to be used effectively in ultra-precision manufacturing process too: (1) Using specific feature extraction and selection methods for systematically designing and selecting suitable features require priori domain knowledge and expert input [15], [16]. In addition, ultra-precision manufacturing has the characteristics of small cutting allowance, less vibration and weak signal features. In ultra-precision manufacturing there is very little research in expert-based feature selection and extraction. Even if there were a significant body of literature, relying on expert knowledge (human expert) would limit the potential use of the system. Autonomous feature extraction and selection would be preferred in this case. (2) In ultra-precision manufacturing it is found that even when the cutting tool exhibits small wear rate the impact on part quality can be significant. In addition, the tool wear process is highly complex and non-linear, thus challenging to identify via methods not developed specifically for ultra-precision machining i.e. methods originally developed for traditional/classical machining [17]-[19].

Compared to traditional Machine Learning and intelligent systems methods, Deep Learning has the most notable advantage of powerful complex non-linear learning ability. The conspicuous difference between DL and shallow learning neural-based methods is that the former can adaptively learn valuable features from original data [20], [24], [25]; autonomous feature extraction and selection is also possible as part of the overall data-driven modelling process.

During the last few years, DL-based models have been developed and applied in intelligent fault diagnosis, especially the gear and bearing fault diagnosis. However, it is known that the performance of deep models largely depends on the original input data (quantity and quality). Thus, choosing TD data [18], [21] or FD data [22], [23] as inputs into DL models for fault diagnosis will have the following challenges: (1) Signals will have different properties in different feature spaces [14]. In fact, the influence of specific input types in different spaces on the performance of DL models is still not clear. (2) Ultra-precision manufacturing processes have the characteristics of very strict cutting tolerance and in general a less pronounced vibration signature. Features extracted from a single feature space in ultra-precision machining may have the limitations of being scarce, which can't meet the requirement for tool condition identification. Thus, it is important to develop a new framework for TCM and create a bespoke Deep Learning model to address multiple feature sets, autonomous feature selection capability, and robust performance suitable for real manufacturing environments.

In this research work it is proposed a multiple feature spaces-based, and bespoke, deep learning-based framework for TCM in ultra-precision manufacturing process. In this study, all the data have been collected from a real manufacturing plant, relevant to shell machining for consumer electronics. The datasets include measurements of vibration and have been preprocessed by FFT and WT to create a preliminary signal set. First, a new 'parallel training model' is designed suitable for three kinds of feature spaces (TD data, FD data and WD data) to learn the low-layer features of the DL structure (feature selection/extraction). Then, a feature fusion model is employed to learn to correlate the high-layer features to tool condition. To achieve the proposed DL structure, and parallel learning, a modified loss function and training framework are used to improve the performance of

the designed DL structure. The contribution of this paper is that via the proposed new DL modeling framework we take advantage of the implicit feature learning ability of deep layer models as well as the characteristics of different feature spaces. Thus, avoiding the dependence on human-assisted feature identification and over-reliance on expert knowledge. Results show that the proposed modeling framework outperforms existing Machine Learning model-based methods for TCM, as well as standard deep learning methods in terms of both accuracy and robustness. In addition, the influence of the input in different feature spaces on the performance of deep models as well as other established ML methods is discussed to further exemplify the effectiveness of the proposed modeling framework.

The rest of this paper is organized as follows: After introducing the required background on ultra-precision manufacturing as well as the application of ML on machining, background theory on SAE is presented in Section II. In Section III, the proposed modeling framework is detailed, as well as its application for TCM in ultra-precision manufacturing. The experimental validation setup, including the data acquisition, are detailed in Section IV. In Section V, the experimental results are discussed which includes comparative analysis and discussion. Finally, the conclusion and future work are summarized in Section VI.

II. Deep Learning Framework

A. The dimension reduction principle based on sparse auto-encoder (SAE)

Schölkopf et al. [26] proposed an unsupervised feature learning theory based on sparse representations. Given an input, it uses an encoder and decoder preceded by a non-linearity that transforms a code vector into a sparse output vector, with both vectors being as similar as possible to the input.

The SAE theory is based on two main components:
1) The **encoder**: Given a signal data $X \in \mathbf{R}^n$, it uses a random matrix W and all ones bias vector b to obtain a sparse-compressed representation $Y \in \mathbf{R}^m (m << n)$ via nonlinear sigmoid function.
2) The **decoder**: the sparse representation Y is transformed back to a reconstruction vector $Z \in \mathbf{R}^n$ via the *sigmoid* function.

The target is to find the optimal parameters *W and b* to minimize the distance between the reconstruction vector *Z* and the input vector *X*. Full details on the SAE model can be found in [27].

B. Stacked SAE

A stacked sparse autoencoder (SSAE) is constructed with the input layer and the hidden layer of several sparse autoencoders, which can extract deeper and more implicit features than a single auto-encoder. The description of the training structure follows:

$$Y^{(k)} = f_s \left(W^{(k)} X^{(k)} + b^{(k)} \right) \tag{1}$$

$$X^{(k+1)} = Y^{(k)} \tag{2}$$

where $W^{(k)}, b^{(k)}, X^{(k)}, Y^{(k)}$ are weight matrix, bias vector, the input and the sparse representation of the *k*-th sparse autoencoder in the encoding procedure.

The loss function of the standard SSAE model is defined as follows [28]

$$J_{sparse}(W,b) = J(W,b) + \beta \sum_{j=1}^{s_2} KL\left(\rho \| \hat{\rho}_j\right) \tag{3}$$

$$J(W,b) = \left[\frac{1}{m}\sum_{i=1}^{m}\left(\frac{1}{2}\left\|h_{W,b}\left(x^{(i)}\right) - y^{(i)}\right\|^2\right)\right] + \frac{\lambda}{2}\sum_{l=1}^{n_l-1}\sum_{i=1}^{s_l}\sum_{j=1}^{s_{l+1}}\left(W_{ji}^{(l)}\right)^2 \tag{4}$$

$$KL\left(\rho \| \hat{\rho}_j\right) = \rho\log\frac{\rho}{\hat{\rho}_j} + (1-\rho)\log\frac{1-\rho}{1-\hat{\rho}_j} \tag{5}$$

where *x* is the original input and *y* the corresponding label; *m* is the number of samples and *n* is the number of the layers; λ, β and ρ are the regularization constant, divergence constant and sparseness constant, respectively; $\hat{\rho}$ is the mean activation value.

III. Proposed FMSSAEs-Based Method For Tool Condition Monitoring

A. The novel FMSSAEs structure

1) Parallel Training Based On Multiple Stacked Sparse Autoencoders

Using a single feature space is popular in the application of fault diagnosis, and in particular via the use of deep learning methods [18], [23]. However, different feature spaces in the vibration signal may have valuable and implicit information; existing DL methods do not simultaneously extract information from multiple spaces to characterize tool wear in machining. Moreover, in ultra-precision machining, signals and features are faint and inconspicuous, which could lead to poor overall performance of tool condition monitoring. Thus, this paper proposes a parallel training model formed by using TD data, FD data, and WD data of the original vibration signal as the input of three different stacked sparse autoencoders to improve the capability of capturing different features in different spaces and implicit information.

Fig. 1 represents the feature learning process of the proposed parallel training model based on multiple stacked sparse autoencoders. The structures of the three stacked sparse autoencoders consist of the same number of network layers as well as hidden and output nodes. The input of the visible layer consists of the raw TD data $X_1 \in \mathbf{R}^{N_1}$, the FD data $X_2 \in \mathbf{R}^{N_2}$ following application of FFT and the WD data $X_3 \in \mathbf{R}^{N_3}$ following a wavelet transform. Each hidden layer is divided into three groups $H_{1k}, H_{2k}, H_{3k} \in \mathbf{R}^{M_k}$. Through calculation and sparse representation of several stacked sparse autoencoders, via the proposed framework three different goal representations will be obtained Y_1, Y_2 and Y_3. The learning process of any one of three stacked sparse autoencoders is independent of the others.

As it can be seen in the structure presented in **Fig. 1** the parallel training model makes no use of any labels, which is different from most standard deep learning models that use labeled data to perform supervised learning. Thus, the loss function of the model in this subsection is modified as

$$J^i_{j\,sparse}\left(W^i_j, b^i_j\right) = J^i_j\left(W^i_j, b^i_j\right) + \beta^i \sum_{k=1}^{t^i_j} KL\left(\rho^i \parallel \hat{\rho}^i_{k,j}\right) \quad (6)$$

$$J^i_j\left(W^i_j, b^i_j\right) = \frac{1}{2m}\sum_{h=1}^{m}\parallel f_s\left(W^{'i}_j f_s\left(W^i_j X^{i,h}_j + b^i_j\right) + b^{'i}_j\right) - X^{i,h}_j \parallel^2 + \frac{\lambda^i}{2}\sum_{r=1}^{j}\sum_{s=1}^{s^i_j}\sum_{t=1}^{t^i_j}\left(W^{i,r}_{ts}\right)^2 \quad (7)$$

$$W^i_j, b^i_j = \arg\min\left\{J^i_{j\,sparse}\left(W^i_j, b^i_j\right)\right\} \quad (8)$$

where $i = 1,2,3$ and j are the i-th SSAE and the j-th sparse autoencoder accordingly. W, b and W', b' are the weight matrix and the bias vector of the encoding and decoding process, respectively. X is the input vector. s and t are the number of nodes.

The optimal solution of the weight matrices W^i_j and the bias vectors b^i_j can be calculated by using (6-8). And the target representation Y_1, Y_2 and Y_3 are obtained after parallel training.
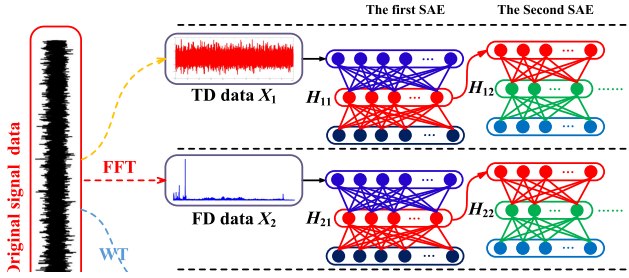

Fig. 1. The feature learning process of the parallel training model.

2) Study on Feature Fusion Based On the Parallel Training Model

After transforming the representation Y_1, Y_2 and Y_3 into a new feature vector $X_F = [Y_1\ Y_2\ Y_3]$, the vector will be used as the input for the next phase of our training framework, which consists of another SSAE. The difference between the fusion model and the parallel training model is that the fusion model makes use of labeled data.

Fig. 2 represents the learning and back propagation process of the fusion model. First, the feature $X_F \in \mathbf{R}^{X_f}$ is used as input to the SSAE, and the first hidden representation $H_1 \in \mathbf{R}^{H_1}$ can be calculated by the weight matrix $W_1 \in \mathbf{R}^{H_1 \times X_f}$ and *sigmoid* function f_S. Subsequently, the second hidden representation $H_2 \in \mathbf{R}^{H_2}$ can be calculated by the weight matrix $W_2 \in \mathbf{R}^{H_2 \times H_1}$ and f_S. The error E_1 between H_2 and the labels $y \in \mathbf{R}^{H_2}$ will also be calculated in this phase. The weight matrix W_2 will be fine-tuned into w_2 based on E_1, and then W_1 will be updated into w_1 based on w_2 and E_1. The hidden representation H_1 are transformed into H'_1 based on X_F and w_1. And then, the output vectors X'_F can be calculated by H'_1 and w_1. Finally, the error E_2 between X'_F and X_F input is used into the parallel training model for the purpose of the error back propagation, as detailed in the next section.

3) Training Rules and Error Propagation

To have better convergence and reconstruction ability as well as deeper features, the proposed FMSSAEs framework makes use of an enhanced learning regime that involves: twice the training and twice the fine-tuning on each learning iteration. Thus, the loss function needs to be modified accordingly.

The learning process of the model is demonstrated as follows: First, the raw TD data X_1, FD data X_2 and WD data X_3 are used as the input vectors to the parallel training model, to capture the target representations Y_1, Y_2 and Y_3 respectively. As a second step, the target representations are transformed into a new feature vector $X_F = [Y_1\ Y_2\ Y_3]$, which is subsequently used to obtain the hidden representation H_2, via another SSAE. On the third step, the first (of the two) fine-tuning processes will be carried out in the fusion model based on the error E_1 between H_2 and the labels y and the loss function $J_{sparse2}\left(W_p, B_p\right)$. And finally, the second fine-tuning will be carried out in the parallel training model based on the error E_2 between X'_F and X_F and the loss function $J^i_{j\,sparse1}\left(W^i_j, B^i_j\right)$.

The above described training function is summarized as follows

$$J_{sparse2}\left(W_p, B_p\right) = J_2\left(W_p, B_p\right) + RL + \beta \sum_{q=1}^{N_{p+1}} KL\left(\rho \parallel \hat{\rho}_{p,q}\right) \quad (9)$$

$$J_2\left(W_p, B_p\right) = \begin{cases} \dfrac{1}{2m}\sum_{q=1}^{m}\left\| f_{\left(W_p, B_p\right)s}\left(x^{(q)}_p\right) - Labels^{(q)} \right\| & p = n-1 \\ \dfrac{1}{2m}\sum_{q=1}^{m}\left\| f_{\left(W_{p+1}, B_{p+1}\right)s}\left(x^{(q)}_p\right) - f_{\left(w_{p+1}, b_{p+1}\right)s}\left(x^{(q)}_p\right) \right\|^2 & p = n-2,\ldots,1 \end{cases} \quad (10)$$

$$RL = \frac{\lambda}{2}\sum_{k=1}^{n_k-1}\sum_{m=1}^{s_k}\sum_{n=1}^{s_{k+1}}\left(W^{(k)}_{nm,p}\right)^2 \quad (11)$$

$$w_p, b_p = \arg\min\left\{J_{sparse2}\left(W_p, B_p\right)\right\} \quad (12)$$

$$J^i_{j\,sparse1}\left(W^i_j, B^i_j\right) = J^i_j\left(W^i_j, B^i_j\right) + RL_j + \beta \sum_{k=1}^{N^i_j} KL\left(\rho \parallel \hat{\rho}^{i,k}_j\right) \quad (13)$$

$$J^i_j\left(W^i_j, B^i_j\right) = \begin{cases} \dfrac{1}{2m}\sum_{h=1}^{m}\left\| f_{\left(W^i_j, B^i_j\right)s}\left(x^{i,(h)}_j\right) - Y^{i,(h)}_j \right\|^2 & i = n_j-1 \\ \dfrac{1}{2m}\sum_{h=1}^{m}\left\| f_{\left(W^{i+1}_j, B^{i+1}_j\right)s}\left(x^{i+1,(h)}_j\right) - f_{\left(w^{i+1}_j, b^{i+1}_j\right)s}\left(x^{i+1,(h)}_j\right) \right\|^2 & i = n_j-2,\ldots,1 \end{cases} \quad (14)$$

$$RL_j = \frac{\lambda}{2}\sum_{r=1}^{n_j-1}\sum_{s=1}^{N^i_j}\sum_{t=1}^{N^{i+1}_j}\left(W^r_{j,ts}\right)^2 \quad (15)$$

$$w^i_j, b^i_j = \arg\min\left\{J^i_{j\,sparse1}\left(W^i_j, B^i_j\right)\right\} \quad (16)$$

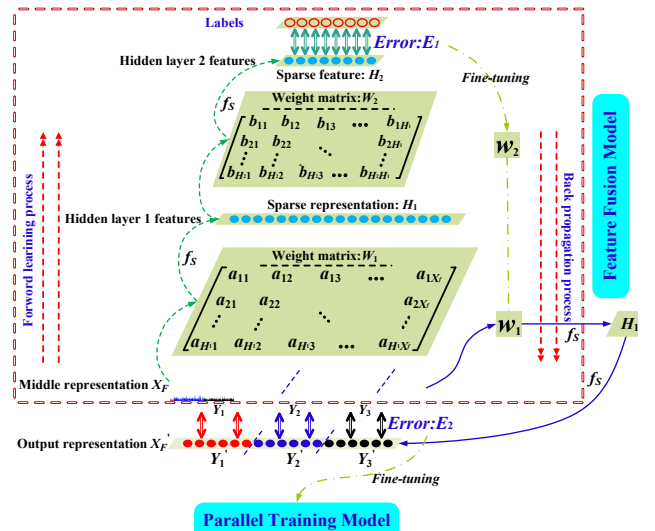where m is the number of samples; n and n_j are the layer

Fig. 2. The learning and back propagation process of the feature fusion model.

number of the fusion model and the parallel training model respectively. N is the number of nodes.

B. Algorithmic procedure for proposed methodology

To apply the proposed FMSSAE modeling framework to the case study of ultra-precision machining the following data processing and algorithmic process is followed:

1) First, the vibration signal of the tool in ultra-precision machining is collected from the manufacturing facility. Next, the TD data X_1, FD data X_2 and WD data X_3 are captured by pre-processing the signal via FFT and WT. Subsequently, all the data are divided into the training and testing samples based on the labels which have been recorded by measuring the surface quality of the finished workpieces. This is for the purpose of model validation.

2) The target representations Y_1, Y_2 and Y_3 of the training samples are extracted via the unsupervised parallel training model and converted to a feature vector X_F.

3) Construct the fusion model based on the inputs/features out of the parallel training model. The fusion model is used for feature learning of the feature vector. The learned deep features H_2 are fed into a BP algorithm for fine-tuning the parameters W and b of the fusion model based on the labels y in a supervised learning fashion.

4) The parameters W^i and b^i of the parallel training model are updated based on step 3) that the parameters of the fusion model have been updated.

5) In the FMSSAEs modeling framework steps 3) and 4) will be repeated iteratively to train the overall model until the framework reaches the intended iterative steps. And finally using the testing samples to validate the performance of the proposed model, in addition, verify the generalization of the proposed method.

IV. EXPERIMENT SETUP AND DATA SET ACQUISITION

A. Experiment setup

In this research study, vibration data are collected continuously from a JDLVM550T_A13S CNC machine tool that is used to machine the external shell of a portable electronic device in a production line, i.e. a real manufacturing environment. **Fig.3** depicts the cutting tools experimental setup for ultra-precision machining and the data acquisition system. The machine tool is used to process and shape the external shell. The accelerometer with sensitivity of 100.9 mv/g is mounted on the spindle seat of the machine tool for measuring the x-direction vibration signals. The vibration signals were collected at a sampling frequency of 10 kHz, and the overall sampling time is 20 seconds. The feed rate is set at 800 mm/min, and the spindle speed at 5500 rpm. Based on the parameters and the spindle speed (v_s), the characteristic frequency ($f = v_s / 60$) of the cutting tool can be calculated.
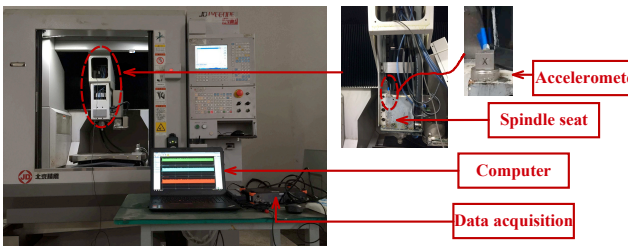

Fig. 3. The cutting tools experimental setup for ultra-precision machining.

B. Data acquisition

The data acquisition is described in the following points:

Firstly. All the data acquisition is performed at the manufacturing environment, not the laboratory.

Secondly. For consistency, all the workpieces are machined under the same cutting parameters. In order to indirectly evaluate the tool condition (for the purpose of sample labeling and supervised learning), the surface quality of each finished workpiece is measured under an Olympus microscope STM6 at a magnification of ×1000.

Thirdly. Three cutting tools were assessed for this study (tool A, B and C) for the purpose of experiment validation and generalization verification. The parameters for the cutting tools are listed in **Table I**. There's a slight difference in the tool setup parameters, which represents how the tools are used in a real manufacturing environment. These differences are to account for various uncertainties in the manufacturing process, and yield a different number of parts processed by each tool. While the manufacturing cell continuously records data, some samples are randomly selected for training, and the remaining for testing the proposed modeling framework.

In the experimental process, four different surface quality states have been defined on the finished workpieces, corresponding to four kinds of gradual tool wear conditions: Initial wear, Normal wear, Rapid degradation and Severe degradation. This categorization also matches expert knowledge on the particular mechanisms of tool wear for the process under investigation. **Fig. 4** depicts the four surface quality states and the tool wear conditions under the microscope magnifying ×1000 and ×700, respectively.

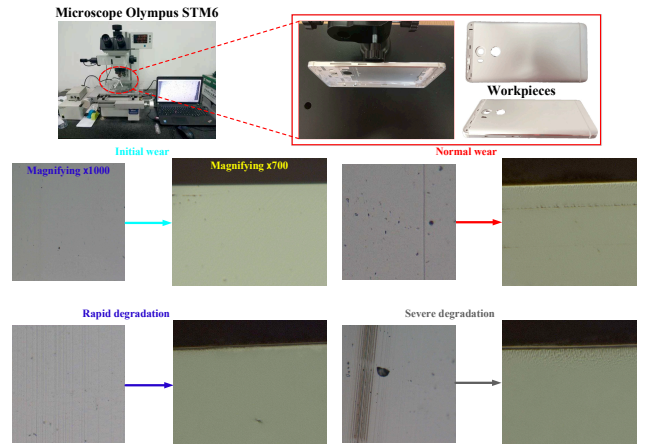Fig.4. The four surface quality states and the tool wear conditions under the microscope magnifying ×1000 and ×700.

TABLE I
PARAMETERS OF THE CUTTING TOOLS

Work material	Tool material	Tool number	Relief angle	Flank width	Maximum workpiece number	Cutting allowance
Aluminium alloy	Diamond	A	3.1°	69.8mm	596	0.01mm
		B	3.4°	71.8mm	593	
		C	4.7°	91.8mm	436	

TABLE II
DESCRIPTION OF THE CUTTING TOOLS WEAR CONDITIONS

Wear conditions of the cutting tools	Size of samples				Label of conditions
	Tool A	Tool B	Tool C	Total	
Initial wear	64	54	43	161	1
Normal wear	307	306	204	817	2
Rapid degradation	138	132	105	375	3
Severe degradation	87	101	84	272	4

Table II shows the size of sample sets and the label of conditions. Each condition contains 161, 817, 375, and 272 samples, respectively. Each sample is a raw vibration signal containing 20 thousand data points following some filtering to remove noise. Meanwhile, FFT and WT are applied to each sample signal in order to obtain FD and WD data. Therefore, the raw data, FD data and WD data contains 20000, 16285 and 20000 data points, respectively. Because of the strict cutting tolerances and less overall vibration in ultra-precision machining (compared to normal machining), the amplitude of the raw vibration signal of the four health conditions is quite similar, on first inspection, as shown in **Fig. 5**.
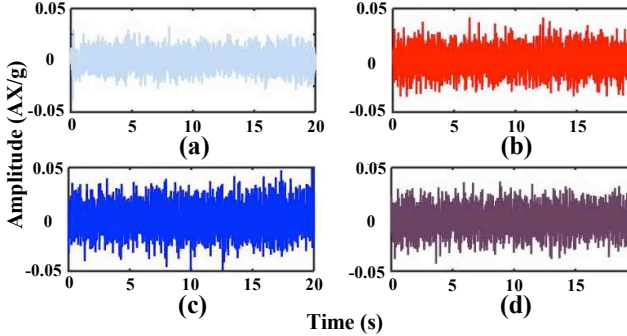

Fig.5. Amplitudes of the raw vibration signal of the four wear conditions. (a) Initial wear. (b) Normal wear. (c) Rapid degradation. (d) Severe degradation.

V. EXPERIMENT RESULTS

A. Comparison to established ML methods

BPNN and SVM are widely used for tool condition monitoring and fault diagnosis, as discussed in the introduction section. However, these Machine Learning, or intelligent systems, methods often rely on engineering experience and expert knowledge to artificially design and extract features, which are not trivial tasks in the whole modeling workflow. In this section a comparison is made between BPNN with a shallow layer structure and an SVM structure against the proposed method.

TABLE III
DESCRIPTION OF THE PARAMETERS OF THE TRADITIONAL METHODS

Description	Parameters	
The traditional methods	BPNN	SVM
Transfer function	logsig	-
Kernel function	-	linear
Penalty parameters	-	0.25
Learning rate	0.8	-
Momentum constant	0.9	-
Epochs	700	700

Different feature spaces in the original signal may have different properties each, hence will pose a different challenge to any data-driven modeling framework. For comparison purposes the performance of BPNN and SVM will be discussed based on the TD feature space, and also the FD feature space, as well as the fusion/combination of the two. A number of statistical features from time domain (Mean, Standard deviation, Skewness factor, etc.) and frequency domain (Variance, Kurtosis factor, etc.) are extracted, more details can be found in [3], [30]. **Table III** shows the model parameters for the BPNN and SVM model structures. The average identification accuracy and the standard deviation comparison of the different methods and features using 10 experiments are listed in **Table IV**, and the detailed modeling results are shown in **Fig. 6**.

In **Table IV** results show that, among the different methods, the proposed method has the best performance (average accuracy: 96.63%, standard deviation: 0.007242), which is superior to the traditional ML methods (best result: 91.97%, 0.008259). In terms of the different methods based on different spaces, SVM with the fusion features exhibits the better performance (average accuracy: 91.91%) compared to
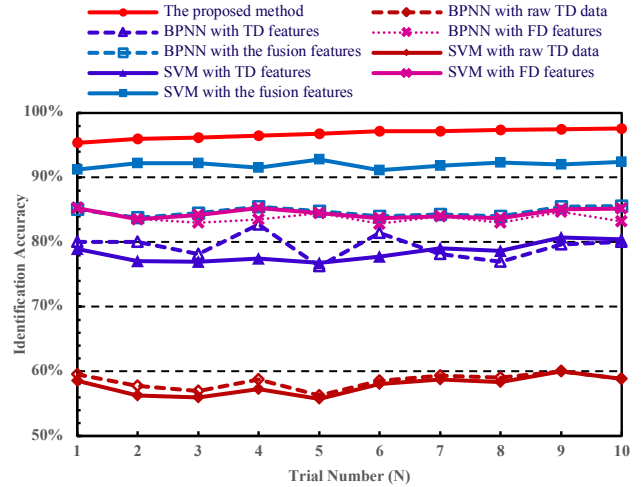

Fig. 6. Identification results of the 10 trials using different methods.

IDENTIFICATION RESULTS OF DIFFERENT METHODS

Methods	Average testing accuracy	Standard deviation
The proposed method	**96.63% (3503/3625)**	**0.007242**
BPNN with raw TD data	58.51% (2118/3625)	0.011796
BPNN with TD features	79.34% (2878/3625)	0.019776
BPNN with FD features	83.77% (3038/3625)	0.008259
BPNN with the fusion features	84.70% (3069/3625)	0.009812
SVM with raw TD data	57.76% (2088/3625)	0.014111
SVM with TD features	78.39% (2835/3625)	0.014092
SVM with FD features	84.45% (3061/3625)	0.009059
SVM with the fusion features	91.97% (3333/3625)	0.008334

TABLE V
THE NETWORK PARAMETERS OF DIFFERENT DEEP LEARNING METHODS

Deep learning methods	Structure	Input	Layers	Nodes number	Learning rate	Iteration
The proposed method	Parallel learning model	TD data	4	20000-1870-187-41	0.8	700
		FD data	4	16385-1870-187-41	0.8	700
		WD data	4	20000-1870-187-41	0.8	700
	Fusion model	The fusion features	3	123-20-4	0.8	700
Standard SAE	-	TD data	4	20000-1870-187-41	0.8	700
	-	FD data	4	16385-1870-187-41	0.8	700
	-	WD data	4	20000-1870-187-41	0.8	700

BPNN (average accuracy: 84.70%). This is still inferior to the proposed method of parallel processing the feature spaces.

In **Fig. 6** results show that, from the first trial to the last trial, with the increase of the training samples, the accuracy of the proposed method keeps growing, which is typical of continuous learning in DL networks.

Another interesting observation is that following the same use of features BPNN and SVM have similar performance such as when using raw data and TD features, especially in terms of the average accuracy.

These results indicate that: (1) Compared with established ML methods (BPNN and SVM), the proposed method shows great advantages, which includes the ability to separately extract features autonomously despite the complexity and dimensionality of the feature space set, due to its deep layer structure and non-linear mapping ability. (2) The traditional methods depend on human-assisted feature extraction. From **Table IV** it can be seen that if the selected feature set is uncorrelated to the labels, the model will show poor accuracy in classifying tool wear. (3) From the first trial to the last trial, the accuracy of BPNN and SVM keeps fluctuating, as expected, due to the batch training process. The DL framework takes advantage of inherent sequential training to improve its overall prediction accuracy.

B. Results in different features spaces

In recent years, due to advances and access to significant computational power, DL methods have been applied to gear and bearing fault diagnosis. However, the influence of different feature spaces on DL methods is still unclear in fault detection. In order to further scrutinize the performance of the proposed FMSSAEs model, the effectiveness of the model and the different feature spaces on comparable DL methods will be studied and surveyed via several experimental trials. **Table V** describes the structure of the studied DL methods for features extraction. In this section, results will be discussed for the following three different feature sets: the TD data, FD data and WD data.

The average identification accuracy and the standard deviation of the different feature spaces on DL methods are listed in **Table VI**, and the detailed results with 10 experiments in each trial are shown in **Fig. 7**. It can be concluded that the identification accuracy of separate feature spaces on deep learning methods vary considerably. Among them, the proposed method with data fusion has the best performance (average accuracy: 96.63%, standard deviation:

0.007242), which is superior to standard DL methods with single feature space (best result: 90.04%, 0.010881).

The reconstruction error curves of the SAE model based on the different inputs and the proposed method are shown in **Fig. 9**. Although the proposed DL model needs more training time (above 4 minutes) due to the increase of units and network layers, the reconstruction error is smaller following convergence. Meanwhile, the variability of the weight update can be reflected on the reconstruction curve, which is an indicator of efficient training.

Fig. 8 represents the details identification accuracy of all the methods based on different training samples. The results indicate that the more the training sample sizes the better the performance of all DL methods (which is expected), while the traditional methods have no such characteristic.

The above results imply that: (1) *Feature selection and extraction*. The traditional ML methods depend on artificial feature extraction via expert knowledge while DL methods have the advantages of autonomous selection of implicit representation through non-liner mapping. There may be equally good combinations of selecting the feature set (compared to the autonomous method) for the traditional ML methods, but this would require tedious and laborious processes to find out. (2) *Generalization ability*. The performance of DL methods can get better accuracy with the
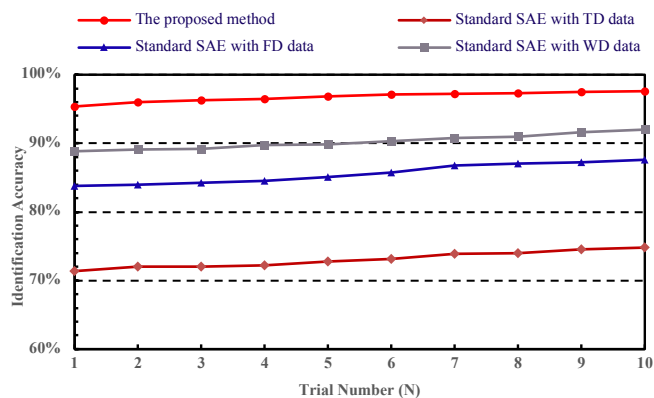

Fig. 7. Identification results of the 10 trials using different feature spaces on DL methods.

TABLE VI
THE INFLUENCE OF DIFFERENT FEATURE SPACES ON DL METHODS

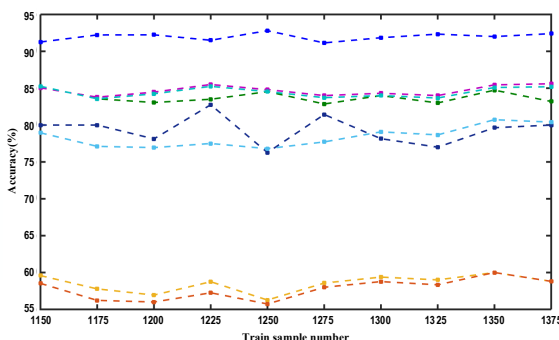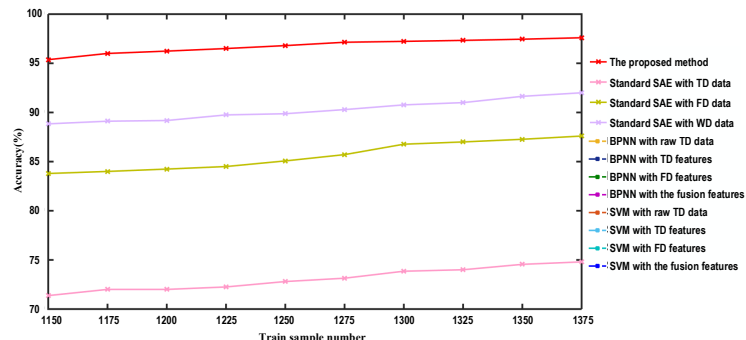| Deep learning methods	Input	Average testing accuracy	Standard deviation
The proposed method	**Data fusion**	**96.63% (3503/3625)**	**0.007242**
	TD data	72.86% (2641/3625)	0.011826
Standard SAE	FD data	85.32% (3093/3625)	0.014646
	WD data	90.04% (3264/3625)	0.010881

Fig. 8. The details results of all the methods based on different training samples.
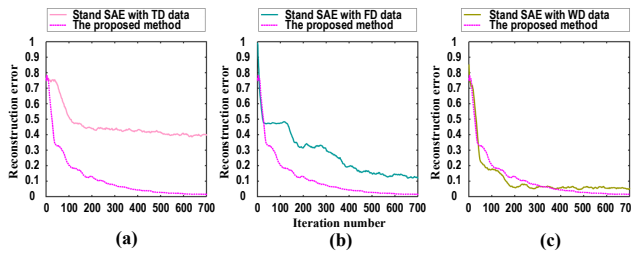
Fig. 9. The reconstruction error curves of deep learning algorithms based on different feature spaces.

increase of the training samples while the traditional methods do not have this property. This shows that the DL methods can get better results if there are sufficient samples, which is somewhat expected due to the complexity of the DL structure. (3) *Model performance*. The proposed method is superior to the established popular ML methods, often used in tool wear prediction, as well as compared to DL methods due to the modified loss function and enhanced training algorithm that takes advantage of separate feature spaces to extract features, but combines them to link them to the labeled outcomes (tool wear).

C. Generalization verification

In this section, the data sets of tool A, B and C are used to further scrutinize (beyond using testing data from the same tool) the generalization ability of the proposed modeling framework. The acquired data samples are separated into two parts: the training sets (tool A and B) used for model training and the testing sets (tool C) for assessing generalization.

Fig. 10. (b) represents the RMS of the vibration signal of tool C (During the 1st workpiece to the 436th workpiece) and the four kinds of tool operation conditions, which are initial wear stages, normal wear stages, rapid degradation and severe degradation. **Table VII** shows the training sets, testing sets and the input features of the three methods.

Fig. 10 (a) shows the prediction performance of the testing sets. It can be observed that the proposed method shows very good generalization properties for TCM in ultra-precision machining. In addition, **Table VII** reveals that the proposed
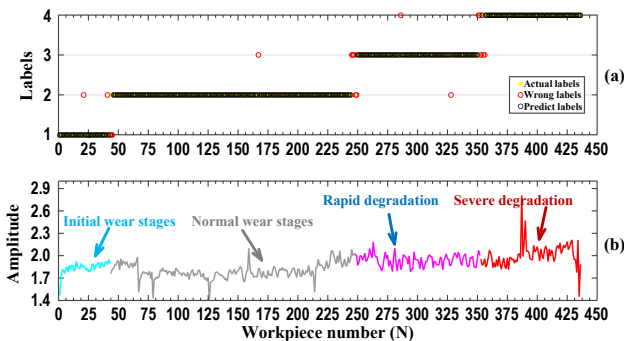

Fig. 10. Identification results of the proposed method on tool C data set.

TABLE VII
IDENTIFICATION RESULTS OF DIFFERENT METHODS

Methods	Training sets Tool A	Tool B	Testing sets Tool C	Input	Testing accuracy
The proposed method				Multiple features spaces-based	93.18% (406/436)
Standard SAE	596	593	436	WD data	86.82% (378/436)
SVM				14 TD features and 11 FD features	88.24% (385/436)

methodology outperforms standard SAE DL as well as and traditional SVM method in terms of identification accuracy. These positive results demonstrate that the proposed methodology can potentially be used in a real manufacturing environment, to accurately identify tool wear states for TCM in ultra-precision manufacturing.

VI. CONCLUSION AND FUTURE WORK

In this paper, a novel multiple feature spaces-based deep learning model (FMSSAEs) is proposed for tool condition identification in ultra-precision manufacturing. Firstly, a new parallel training model structure is designed to learn the low-layer features in terms of feature extraction and selection. Then, a fusion model is employed to learn the deep features and fine-tune the parallel training model to further adjust the network's parameters. To achieve this structure, the proposed method makes use of a modified loss function and an improved overall training framework.

The proposed method is applied to real manufacturing data, consisting of cutting tool vibration signals captured during an ultra-precision machining process. Results show that the proposed method is more effective compared to established and popular ML methods for tool wear prediction, as well as standard deep learning methods used for tool condition monitoring. Generalization properties appear to be good on the new proposed methodology, however, there are certain limitations when a different tool is used because of the variability in setup tool parameters of the different cutting tools, such as relief angle, flank width, etc. Further research work is needed in this area, to perhaps focus the model training regime on creating uncertainty tolerant features, rather than aim for ultimate overall prediction accuracy.

With the rapid development of hardware technology and computational power, deep learning structures can find application in more industrial field, however modification and enhancement of the DL framework to suit a particular application, including efficient error propagation and heuristic training regime, are not trivial tasks.

REFERENCES

[1] L. B. Kong, C. F. Cheung, W. B. Lee and S. To, "An Integrated Manufacturing System for the Design, Fabrication, and Measurement of Ultra-Precision Freeform Optics," *IEEE Transactions on Electronics Packaging Manufacturing*, vol. 33, no. 4, pp. 244–254, Oct. 2010.

[2] A. J. Torabi, M. J. Er, X. Li, B. S. Lim and G. O. Peen, "Application of clustering methods for online tool condition monitoring and fault diagnosis in high-speed milling processes," *IEEE Systems Journal*, vol. 10, no. 2, pp. 721–732, Jun. 2016.

[3] N. Li, Y. J. Chen, D. D. Kong and S. L. Tan, "Force-based tool condition monitoring for turning process using v-support vector regression," *International Journal of Advanced Manufacturing Technology*, vol. 91, pp. 351–361, Jul. 2017.

[4] M. S. H. Bhuiyan and I. A. Choudhury, "Review of sensor applications in tool condition monitoring in Machining," *Comprehensive Materials Processing*, vol. 13, pp. 539–569, Apr. 2014.

[5] C. H. R. Martins, P. R. Aguiar, A. Frech, and E. C. Bianchi, "Tool condition monitoring of single-point dresser using acoustic emission and neural networks models," *IEEE Transactions on Instrumentation and Measurement*, vol. 63, no. 3, pp. 667–679, Mar. 2014.

[6] O. Geramifard, J.X. Xu, J.H. Zhou and X. Li, "A physically segmented hidden Markov model approach for continuous tool condition monitoring: diagnostics and prognostics," *IEEE Transactions on Industrial Informatics*, vol. 8, no. 4, pp. 964–973, Jun. 2012.

[7] K. Patra, "Acoustic emission based tool condition monitoring system in drilling," *Lecture Notes in Engineering and Computer Science*, vol. 3, no. 1, pp. 2126–2130, 2011.

[8] X. C. Ku, Y. M. Zhou, P. L. Gao and M. D. Duan, "Recognition of tool wear state based on wavelet packet and BP neural network," *Modern Manufacturing Engineering*, vol. 12, pp. 68–72, 2014.

[9] F. A. Niaki, D. Ulutan and L. Mears, "Wavelet based sensor fusion for tool condition monitoring of hard to machine materials," *International Conference on Multisensor Fusion and Integration for Intelligent Systems*, pp. 271–276, Oct. 2015.

[10] O. Massol, X. Li, R. Gouriveau, J. H. Zhou and O. P. Gan, "An exTS based neuro-fuzzy algorithm for prognostics and tool condition monitoring," *International Conference on Control Automation Robotics and Vision*, pp. 1329–1334, Feb. 2011.

[11] Q. Ren, M. Balazinski, L. Baron, K. Jemielniak, R. Botez and S. Achiche, "Type-2 fuzzy tool condition monitoring system based on acoustic emission in micromilling," *Information Sciences An International Journal*, vol. 255, no. 1, pp. 121–134, Jan. 2014.

[12] Y. Qiu and F.Y. Xie, "Tool wear monitoring based on wavelet packet coefficient and hidden Markov model," *Machine Tool and Hydraulics*, vol. 12, pp. 40–44, 2014.

[13] D. F. Shi and N. N. Gindy, "Tool wear predictive model based on least squares support vector machines," *Mechanical Systems and Signal Processing*, vol. 21, no. 4, pp. 1799–1814, May. 2007.

[14] J. J. Wang, J. Y. Xie, R. Zhao, K. Z. Mao and L. B. Zhang, "A New Probabilistic Kernel Factor Analysis for Multisensory Data Fusion: Application to Tool Condition Monitoring," *IEEE Transactions on Instrumentation and Measurement*, vol. 65, no. 11, pp. 2527–2537, Jul. 2016.

[15] R. Zhao, D. Z. Wang, R. Q. Yan, K. Z. Mao, F. Shen and J. J. Wang, "Machine health monitoring using local feature-based gated recurrent unit networks," *IEEE Transactions on Industrial Electronics*, vol. PP, no. 99, pp. 1–1, Jul. 2017.

[16] E. Kannatey-Asibu, J. Yum and T. H. Kim, "Monitoring tool wear using classifier fusion", *Mechanical Systems and Signal Processing*, vol. 85, pp. 651–661, Feb. 2017.

[17] C. Shang, F. Yang, D. X. Huang and W. X. Lyu, "Data-driven soft sensor development based on deep learning technique," *Journal of Process Control*, vol. 24, no. 3, pp. 223–233, Mar. 2014.

[18] Y. G. Lei, F. Jia, J. Lin, S. B. Xing and S. X. Ding, "An intelligent fault diagnosis method using unsupervised feature learning towards mechanical big data," *IEEE Transactions on Industrial Electronics*, vol. 63, no. 5, pp. 3137–3147, Jan. 2016.

[19] Y. Bengio, A. Courville and P. Vincent, "Representation Learning: A Review and New Perspectives," *IEEE Transactions on Pattern Analysis and Machine Intelligence*, vol. 35, no. 8, pp. 1798–1828, Mar. 2013.

[20] H.D. Shao, H.K. Jiang, H.Z. Zhang, T.C. Liang, "Electric Locomotive Bearing Fault Diagnosis Using a Novel Convolutional Deep Belief Network," *IEEE Transactions on Industrial Electronics*, vol. 65, no. 3, pp. 2727–2736, Aug. 2017.

[21] H. D. Shao, H. K. Jiang, F. Wang and H. W. Zhao, "An enhancement deep feature fusion method for rotating machinery fault diagnosis," *Knowledge-Based Systems*, vol. 119, pp. 200–220, Mar. 2017.

[22] V. T. Tran, F. AlThobiani and A. Ball, "An approach to fault diagnosis of reciprocating compressor valves using Teager-Kaiser energy operator and deep belief networks," *Expert Systems with Applications*, vol. 41, no. 9, pp. 4113–4122, Jul. 2014.

[23] O. Janssens, V. Slavkovikj, B. Vervisch, K. Stockman, M. Loccufier and S. Verstockt, "Convolutional neural network based fault detection for rotating machinery," *Journal of Sound and Vibration*, vol. 377, pp. 331-345, Sep. 2016.

[24] H. Lee, R. Grosse, R. Ranganath and A. Y. Ng, "Convolutional deep belief networks for scalable unsupervised learning of hierarchical representations," *International Conference on Machine Learning*, pp. 609-616, Jun. 2009.

[25] G. E. Hinton and R. R. "Salakhutdinov, Reducing the Dimensionality of Data with Neural Networks," *Science*, vol. 313, no. 5786, pp. 504–507, Jul. 2006.

[26] B. Schölkopf, J. Platt and T. Hofmann, "Efficient Learning of Sparse Representations with an Energy-Based Model," *MIT Press*, pp. 1137–1144, 2007.

[27] J. D. Sun, C. H. Yan and J. T. Wen, "Intelligent Bearing Fault Diagnosis Method Combining Compressed Data Acquisition and Deep Learning," *IEEE Transactions on Instrumentation and Measurement*, vol. 67, no. 1, pp. 185–195, Jan. 2018.

[28] P. Vincent, H. Larochelle, I. Lajoie, Y. Bengio and P.A. Manzagol, "Stacked denoising autoencoders: learning useful representations in a deep network with a local denoising criterion," *Journal of Machine Learning Research*, vol. 11, no. 12, pp. 3371–3408, Mar. 2010.

[29] Y. G. Lei, Z. J. He and Y. Y. Zi, "EEMD method and WNN for fault diagnosis of locomotive roller bearings", *Expert Systems with Applications*, vol. 38, no. 6, pp. 7334-7341, Jun. 2011.

[30] K. Jemielniak, T. Urbański, J. Kossakowska, S. Bombiński, "Tool condition monitoring based on numerous signal features", *International Journal of Advanced Manufacturing Technology*, vol. 59, no. 1-4, pp. 73-81, Mar. 2012.

Chengming Shi is been studying for the Ph.D degree in Mechatronic Engineering for three years already at Huazhong University of science and technology Wuhan, China.

His current research interests include intelligent manufacturing, sensor data mining, signal processing, and machine learning.

George Panoutsos received his PhD degree in automatic control and systems engineering from the University of Sheffield, Sheffield, U.K, in 2007. He joined the Department of Automatic Control and Systems Engineering (University of Sheffield, UK) as a Lecturer in 2010, and he is currently Reader in Computational Intelligence, and Deputy Head of Department. George has a research grant portfolio of over £2M from the UK EPSRC, Innovate UK, EU Horizon 2020 and direct industry funding, as well as over 60 research publications in theoretical as well as applied contributions in the areas of computational intelligence, data-driven modelling, optimization, and decision support systems.

Bo Luo received the Bachelor's degree in Machinery Manufacturing & Automation and the Ph.D. degree in Mechatronic Engineering from Huazhong University of science and technology, Wuhan, China, in 2008 and 2014.

He is currently a postdoctoral researcher with the School of Mechanical Science and Engineering, Huazhong University of Science and Technology. His current research interests include intelligent manufacturing, big data mining, signal processing, and machine learning.

Hongqi Liu received the Ph.D. degree in Mechatronic Engineering from Huazhong University of science and technology, Wuhan, China, in 2008.

He is currently an associate research professor with the School of Mechanical Science and Engineering, Huazhong University of Science and Technology. His current research interests include machinery health monitoring, diagnosis and prognosis, complex systems failure analysis, quality and reliability engineering, and manufacturing systems design, modeling, scheduling, and planning.

Bin Li received the B.S., M.S., and Ph.D. degree in Mechanical Engineering from Huazhong University of science and technology, Wuhan, China, in 1982, 1989 and 2006 respectively. He is currently a professor with the school of Mechanical Science and Engineering, Huazhong University of Science and Technology. His current research interests include intelligent manufacturing and CNC machine tools.
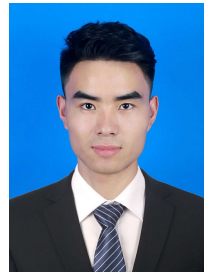
Xu Lin received the M.S. degree in Mechanical Engineering from Huazhong University of science and technology, Wuhan, China, in 2018. His current research interests include intelligent manufacturing, sensor data mining, signal processing and machine learning.